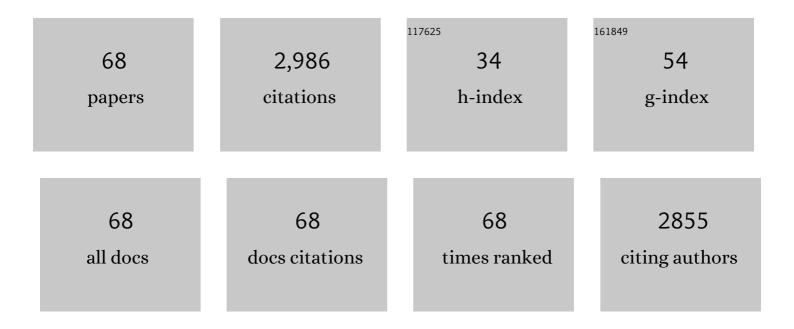
## Marc Debliquy

List of Publications by Year in descending order

Source: https://exaly.com/author-pdf/12098432/publications.pdf Version: 2024-02-01



#	Article	IF	CITATIONS
1	Hydrogen sensors based on noble metal doped metal-oxide semiconductor: A review. International Journal of Hydrogen Energy, 2017, 42, 20386-20397.	7.1	213
2	Room temperature conductive type metal oxide semiconductor gas sensors for NO2 detection. Sensors and Actuators A: Physical, 2019, 289, 118-133.	4.1	143
3	Sensing properties of atmospheric plasma-sprayed WO3 coating for sub-ppm NO2 detection. Sensors and Actuators B: Chemical, 2010, 144, 280-288.	7.8	140
4	Room temperature responses of visible-light illuminated WO3 sensors to NO2 in sub-ppm range. Sensors and Actuators B: Chemical, 2013, 181, 395-401.	7.8	129
5	Graphene-enhanced metal oxide gas sensors at room temperature: a review. Beilstein Journal of Nanotechnology, 2018, 9, 2832-2844.	2.8	126
6	Metal oxide semiconductors with highly concentrated oxygen vacancies for gas sensing materials: A review. Sensors and Actuators A: Physical, 2020, 309, 112026.	4.1	126
7	Room-temperature NO2 gas sensors based on rGO@ZnO1-x composites: Experiments and molecular dynamics simulation. Sensors and Actuators B: Chemical, 2019, 282, 690-702.	7.8	97
8	Hybrid fiber gratings coated with a catalytic sensitive layer for hydrogen sensing in air. Optics Express, 2008, 16, 16854.	3.4	83
9	Sensitive and rapid hydrogen sensors based on Pd–WO3 thick films with different morphologies. International Journal of Hydrogen Energy, 2013, 38, 2565-2577.	7.1	82
10	Sensing mechanism of hydrogen sensors based on palladium-loaded tungsten oxide (Pd–WO3). Sensors and Actuators B: Chemical, 2013, 187, 84-93.	7.8	78
11	Non-enzymatic D-glucose plasmonic optical fiber grating biosensor. Biosensors and Bioelectronics, 2019, 142, 111506.	10.1	77
12	Room temperature gas sensors based on Ce doped TiO2 nanocrystals for highly sensitive NH3 detection. Chemical Engineering Journal, 2022, 444, 136449.	12.7	74
13	Highly sensitive hydrogen sensors based on co-sputtered platinum-activated tungsten oxide films. International Journal of Hydrogen Energy, 2011, 36, 1107-1114.	7.1	71
14	Room-temperature nitrogen-dioxide sensors based on ZnO1â^'x coatings deposited by solution precursor plasma spray. Sensors and Actuators B: Chemical, 2017, 242, 102-111.	7.8	65
15	An ammonia sensor composed of polypyrrole synthesized on reduced graphene oxide by electropolymerization. Sensors and Actuators B: Chemical, 2020, 305, 127423.	7.8	64
16	Visible light enhanced black NiO sensors for ppb-level NO2 detection at room temperature. Ceramics International, 2019, 45, 4253-4261.	4.8	63
17	Molecularly imprinted electropolymerization on a metal-coated optical fiber for gas sensing applications. Sensors and Actuators B: Chemical, 2017, 244, 1145-1151.	7.8	61
18	A Review on Functionalized Graphene Sensors for Detection of Ammonia. Sensors, 2021, 21, 1443.	3.8	61

MARC DEBLIQUY

#	Article	IF	CITATIONS
19	Cadmium sulfide activated zinc oxide coatings deposited by liquid plasma spray for room temperature nitrogen dioxide detection under visible light illumination. Ceramics International, 2016, 42, 4845-4852.	4.8	57
20	Chemically deposited palladium nanoparticles on graphene for hydrogen sensor applications. Scientific Reports, 2019, 9, 3653.	3.3	57
21	Room temperature nitrogen dioxide sensors based on N719-dye sensitized amorphous zinc oxide sensors performed under visible-light illumination. Sensors and Actuators B: Chemical, 2015, 209, 69-77.	7.8	56
22	Low concentration isopropanol gas sensing properties of Ag nanoparticles decorated In2O3 hollow spheres. Journal of Advanced Ceramics, 2022, 11, 379-391.	17.4	56
23	Stability of Metal Oxide Semiconductor Gas Sensors: A Review. IEEE Sensors Journal, 2022, 22, 5470-5481.	4.7	56
24	A Formaldehyde Sensor Based on Molecularly-Imprinted Polymer on a TiO2 Nanotube Array. Sensors, 2017, 17, 675.	3.8	55
25	Deposition and microstructure characterization of atmospheric plasma-sprayed ZnO coatings for NO2 detection. Applied Surface Science, 2010, 256, 5905-5910.	6.1	54
26	H2 sensors based on WO3 thin films activated by platinum nanoparticles synthesized by electroless process. International Journal of Hydrogen Energy, 2013, 38, 2929-2935.	7.1	52
27	Microwave-assisted hydrothermal synthesis of copper oxide-based gas-sensitive nanostructures. Rare Metals, 2021, 40, 1477-1493.	7.1	48
28	High-refractive-index transparent coatings enhance the optical fiber cladding modes refractometric sensitivity. Optics Express, 2013, 21, 29073.	3.4	45
29	Surface Plasmon Resonances in Oriented Silver Nanowire Coatings on Optical Fibers. Journal of Physical Chemistry C, 2014, 118, 11035-11042.	3.1	42
30	Surface plasmon resonance sensing in gaseous media with optical fiber gratings. Optics Letters, 2018, 43, 2308.	3.3	40
31	A Fast and Room-Temperature Operation Ammonia Sensor Based on Compound of Graphene With Polypyrrole. IEEE Sensors Journal, 2018, 18, 9088-9096.	4.7	39
32	Micro-nano structured functional coatings deposited by liquid plasma spraying. Journal of Advanced Ceramics, 2020, 9, 517-534.	17.4	39
33	A novel low-concentration isopropanol gas sensor based on Fe-doped ZnO nanoneedles and its gas sensing mechanism. Journal of Materials Science, 2021, 56, 3230-3245.	3.7	38
34	SO2 Gas Sensors based on WO3 Nanostructures with Different Morphologies. Procedia Engineering, 2012, 47, 1033-1036.	1.2	37
35	Synthesis and NH3/TMA sensing properties of CuFe2O4 hollow microspheres at low working temperature. Rare Metals, 2021, 40, 1768-1777.	7.1	33
36	Sensing properties of Pt/Pd activated tungsten oxide films grown by simultaneous radio-frequency sputtering to reducing gases. Sensors and Actuators B: Chemical, 2012, 175, 53-59.	7.8	30

MARC DEBLIQUY

#	Article	IF	CITATIONS
37	Study of selectivity of NO2 sensors composed of WO3 and MnO2 thin films grown by radio frequency sputtering. Sensors and Actuators B: Chemical, 2012, 161, 914-922.	7.8	30
38	Microstructure and gas sensing properties of solution precursor plasma-sprayed zinc oxide coatings. Materials Research Bulletin, 2015, 63, 67-71.	5.2	30
39	Preparation and characterization of CuxO1-y@ZnO1-α nanocomposites for enhanced room-temperature NO2 sensing applications. Applied Surface Science, 2017, 401, 248-255.	6.1	26
40	Solution precursor plasma-sprayed tungsten oxide coatings for nitrogen dioxide detection. Ceramics International, 2014, 40, 11427-11431.	4.8	25
41	Flexible NO 2 gas sensors based on sheet-like hierarchical ZnO 1â^' x coatings deposited on polypropylene papers by suspension flame spraying. Journal of the Taiwan Institute of Chemical Engineers, 2017, 75, 280-286.	5.3	22
42	Optimization of synthesis parameters of mesoporous silica sol–gel thin films for application on 2024 aluminum alloy substrates. Applied Surface Science, 2013, 277, 201-210.	6.1	21
43	Magnetron sputtered tungsten oxide films activated by dip-coated platinum for ppm-level hydrogen detection. Thin Solid Films, 2012, 520, 3679-3683.	1.8	20
44	Synthesis and acetone sensing properties of copper (Cu2+) substituted zinc ferrite hollow micro-nanospheres. Ceramics International, 2020, 46, 28835-28843.	4.8	20
45	Room-temperature gas sensors based on titanium dioxide quantum dots for highly sensitive and selective H2S detection. Applied Surface Science, 2022, 585, 152744.	6.1	20
46	Role of cobalt in Co-ZnO nanoflower gas sensors for the detection of low concentration of VOCs. Sensors and Actuators B: Chemical, 2022, 360, 131674.	7.8	19
47	Light assisted room-temperature NO 2 sensors with enhanced performance based on black SnO 1-α @ZnO 1-β @SnO 2-γ nanocomposite coatings deposited by solution precursor plasma spray. Ceramics International, 2017, 43, 5990-5998.	4.8	18
48	Hydrothermal Synthesis of Two Dimensional WO3 Nanostructures for NO2 Detection in the ppb-level. Procedia Engineering, 2012, 47, 228-231.	1.2	17
49	Improvement of sensing characteristics of radio-frequency sputtered tungsten oxide films through surface modification by laser irradiation. Materials Chemistry and Physics, 2012, 133, 588-591.	4.0	17
50	Ammonia Sensor Based on Vapor Phase Polymerized Polypyrrole. Chemosensors, 2020, 8, 38.	3.6	14
51	Reversible NO2 Optical Fiber Chemical Sensor Based on LuPc2 Using Simultaneous Transmission of UV and Visible Light. Sensors, 2015, 15, 9870-9881.	3.8	12
52	Past, present, and future trends in boar taint detection. Trends in Food Science and Technology, 2021, 112, 283-297.	15.1	12
53	Visible Light Activated Tungsten Oxide Sensors for NO2 Detection at Room Temperature. Procedia Engineering, 2012, 47, 116-119.	1.2	11
54	Room temperature WO3-Bi2WO6 sensors based on hierarchical microflowers for ppb-level H2S detection. Chemical Engineering Journal, 2022, 430, 132813.	12.7	11

MARC DEBLIQUY

#	Article	IF	CITATIONS
55	Investigation on isopropanol sensing properties of LnFeO3(LnÂ=ÂNd, Dy, Er) perovskite materials synthesized by microwave-assisted hydrothermal method. Applied Surface Science, 2022, 601, 154292.	6.1	10
56	Hydrogen sensors based on Pd-doped WO3 nanostructures and the morphology investigation for their sensing performances optimization. Procedia Engineering, 2011, 25, 264-267.	1.2	8
57	Optical Fibre NO2 Sensor Based on Lutetium Bisphthalocyanine in a Mesoporous Silica Matrix. Sensors, 2018, 18, 740.	3.8	8
58	Comprehensive SPME-GC-MS Analysis of VOC Profiles Obtained Following High-Temperature Heating of Pork Back Fat with Varying Boar Taint Intensities. Foods, 2021, 10, 1311.	4.3	8
59	Infrared radiation detector interrogated by optical frequency-domain reflectometer. Optics and Lasers in Engineering, 2012, 50, 308-311.	3.8	4
60	Low Thermal Conductivity Adhesive as a Key Enabler for Compact, Low-Cost Packaging for Metal-Oxide Gas Sensors. IEEE Access, 2022, 10, 19242-19253.	4.2	4
61	Nanostructured TiO2 Layers for Photovoltaic and Gas Sensing Applications. , 2016, , .		3
62	Facile synthesis of bismuth ferrite nanoparticles for ppm-level isopropanol gas sensor. Journal of Materials Science: Materials in Electronics, 2022, 33, 18507-18521.	2.2	3
63	Nitrogen dioxide sensor based on optical fiber coated with a porous silica matrix incorporating lutetium bisphthalocyanine. , 2013, , .		2
64	Room Temperature NO2 Responses of Visible-Light Activated Nanosheet rGO@ZnO1â^'x Sensors. Proceedings (mdpi), 2017, 1, 411.	0.2	2
65	Using co-sputtered platinum or palladium activated tungsten oxide films to detect reducing gases. Procedia Engineering, 2011, 25, 823-826.	1.2	1
66	N719-dye sensitized amorphous zinc oxide films for NO <inf>2</inf> detection under visible-light illumination. , 2013, , .		1
67	Light-Assisted Room-Temperature NO2 Sensors Based on Black Sheet-Like NiO. Proceedings (mdpi), 2017, 1, 412.	0.2	0
68	Chemical Sensors for VOC Detection in Indoor Air: Focus on Formaldehyde. NATO Science for Peace and Security Series A: Chemistry and Biology, 2019, , 47-70.	0.5	0